

Thus neither e_σ nor e_π for CN^- can be even approximated from this treatment. It is also unrealistic to accept the best-fit ζ values, even when the propagated error turns out to be small, because changes in ζ induce smaller changes in the transition energies than would such factors as the inclusion of additional K^+ (or $[\text{Cr}(\text{CN})_6]^{3-}$) ions in the model.

The value of the Trees parameter, 211 cm^{-1} using the *Pcan* structure, appears large by comparison with the 70-cm^{-1} value for the free Cr^{3+} ion.⁸ Smaller values of the Trees parameter place the ${}^2\text{T}_{2g}$ levels too high in energy when *B* and *C* are chosen to fit the quartets and the ${}^2\text{E}_g$ and ${}^2\text{T}_{1g}$ levels.

The fit to the experimental energies is definitely better for the *Pcan* geometry, but the model includes too many approximations to justify a prediction that this is the structure at 13 K, the temperature at which the excitation spectrum was measured. With either the *Pcan* or *PI* geometry, including a cation field of reasonable magnitude yields a better fit to experiment than no field at all. It is not obvious that this should be so, because at zero cation field the calculated ${}^2\text{T}_{2g}$ splitting is too large, while the ${}^2\text{E}_g$

splitting is too small. If increasing the field increased all splittings monotonically, as many perturbations might be expected to do, the fit would be worse at any value of $e_{\sigma\text{K}}$.

We conclude that it is appropriate to include in any ligand field calculation a field from the counterions. This field appears to be better represented by an AOM parameter $e_{\sigma\text{K}}$ decreasing with R^3 than by an electrostatic parameter I_2 varying in the same manner. The appropriate magnitude of e_σ is $\pm 200\text{--}400\text{ cm}^{-1}$ (for ions $\sim 4\text{ \AA}$ from the metal ion). Whether it is necessary to include the counterion field depends on the symmetry of the counterion sphere. If it is nearly cubic, there will be negligible contributions to the sharp-line splittings, and it would not matter whether it were included or not. The case of a ± 3 chromophore with ± 1 counterions, as represented here, is very likely to produce a counterion environment of lower symmetry, requiring explicit consideration of that environment.

Acknowledgment. We thank the donors of the Petroleum Research Fund, administered by the American Chemical Society, for support of this research. This work was also supported in part by the National Science Foundation under Grant RII8610675. We also thank Prof. Claus Schäffer for helpful comments.

Registry No. $\text{K}_3[\text{Cr}(\text{CN})_6]$, 13601-11-1.

(20) Flint, C. D.; Palacio, D. J. *J. Chem. Soc. Faraday Trans. 2* 1977, 73, 649.

Contribution from the Department of Chemistry,
Harvard University, Cambridge, Massachusetts 02138

Hexanuclear Iron–Sulfur Basket Clusters: Topological Isomers of Prismanes. Synthesis, Structure, and Reactions

Barry S. Snyder and R. H. Holm*

Received December 11, 1987

The new set of cluster molecules $\text{Fe}_6\text{S}_6(\text{PEt}_3)_4\text{X}_2$ ($\text{X} = \text{Cl}^-$ (1), Br^- , I^-) has been prepared by the reaction of $\text{Fe}(\text{PEt}_3)_2\text{X}_2$ (2) with (i) $(\text{Me}_3\text{Si})_2\text{S}$ or Li_2S in THF, (ii) the cubane clusters $[\text{Fe}_4\text{S}_4\text{X}_4]^{2-}$ in acetonitrile, and (iii) the prismane clusters $[\text{Fe}_6\text{S}_6\text{X}_6]^{3-}$ in acetonitrile. Also prepared by similar means were $\text{Fe}_6\text{S}_6(\text{PMe}_3)_4\text{Cl}_2$, $\text{Fe}_6\text{S}_6(\text{PEt}_3)_4\text{Cl}_2$, and $\text{Fe}_6\text{S}_6(\text{P-}i\text{-Bu})_4\text{Cl}_2$ (3). The compounds were obtained as black crystalline solids, usually in purified yields of 50–65%. Precursor complex 2 ($\text{X} = \text{Br}^-$) was isolated as pale yellow crystals with monoclinic space group *Pn*, $a = 7.316$ (1) \AA , $b = 12.316$ (2) \AA , $c = 11.356$ (2) \AA , $\beta = 97.15$ (2)°, and $Z = 2$. The expected (distorted) tetrahedral structure was confirmed, with a notably open Br-Fe-Br angle (121.9 (1)°) presumably set by steric interactions. This angle is one of the largest in the tetrahedral series $\text{M}(\text{PR}_3)_2\text{X}_2$, all of which thus far have X-M-X angles $\geq 105^\circ$; no previous structural data have been reported for type 2 complexes. Compound 3 crystallizes in tetragonal space group *I4*, with $a = 33.78$ (1) \AA , $c = 12.362$ (7) \AA , and $Z = 8$. It contains a $[\text{Fe}_6(\mu_2\text{-S})(\mu_3\text{-S})_4(\mu_4\text{-S})]^{2+}$ core, formally including 2 Fe(III) + 4 Fe(II), and is built by the fusion of six nonplanar Fe_2S_2 rhombs to form an open basket with a bridging group $\text{Fe}(\mu_2\text{-S})\text{-Fe}$ of bond angle 75.5° as the "handle". The core has idealized C_{2v} symmetry with the 2-fold axis containing the $\mu_2\text{-S}$ and $\mu_4\text{-S}$ atoms. Each Fe atom is four-coordinate; the two FeS_3Cl sites have trigonally distorted tetrahedral geometry whereas the four FeS_3P sites resemble very distorted trigonal pyramids with the Fe atoms only ca. 0.11 \AA above the S_3 planes and expanded S-Fe-S angles, one at each site (mean 127.5°), which form edges of the basket and handle in the form of two chairlike Fe_2S_3 rings or "open faces". A simple conceptual relationship among 6-Fe core structures is presented as a scheme wherein different cores are transformed by formal addition (or subtraction) of Fe and S atoms. Arguments based on electrochemical properties are provided to show that basket and prismane ($[\text{Fe}_6(\mu_3\text{-S})_6]$) cores do not interconvert even in the same oxidation level and are therefore topological isomers. The typical cluster 1 exhibits a versatile reaction chemistry that includes unique transformations that result in core conversions. In addition to being formed from $[\text{Fe}_6\text{S}_6\text{Cl}_6]^{3-}$ (4) in a reductive-substitution reaction and from $[\text{Fe}_4\text{S}_4\text{Cl}_4]^{2-}$ (5) in a process of core enlargement and reductive substitution, it is also spontaneously generated in solution from $\text{Fe}_7\text{S}_6(\text{PEt}_3)_4\text{Cl}_3$. Further, in the presence of sulfur and chloride, the phosphines of 1 are removed in the form of Et_3PS in high yield. In acetone solution in the presence of $(\text{Me}_4\text{N})\text{Cl}$, $(\text{Me}_4\text{N})_2[\text{S}]$ was isolated, whereas the use of $(\text{PPN})\text{Cl}$ resulted in isolation of the $(\text{PPN})^+$ salts of 4 and $[\text{Fe}_2\text{S}_2(\text{S}_3)_2]^{2-}$, the latter in low yield. $(\text{PPN})_3[\text{4}]$ could be identified securely only by X-ray crystallography. This compound crystallizes in monoclinic space group *C2/c* with $a = 28.929$ (8) \AA , $b = 15.296$ (5) \AA , $c = 28.898$ (6) \AA , $\beta = 122.39$ (2)°, and $Z = 4$. The anion has a slightly distorted hexagonal prismatic structure with dimensions comparable to those found previously for another salt. In these conversions 85% of the Fe content of 1 is accounted for in the products. The basket and prismane Fe_6S_6 cores are the only open or closed polyhedral cores of this stoichiometry. The open faces of the prismane can be capped by certain metal fragments. These faces of the basket core have the same potential, but their less regular shape and longer $\text{S}\cdots\text{S}$ separations (3.93–4.10 \AA) presumably will require core structural adjustment in the event of formation of a stable capped product.

Introduction

The continuing evolution of iron–sulfur chemistry has resulted in the synthesis of new types of clusters with nuclearities exceeding that of the familiar, biologically relevant cubane-type species containing the $[\text{Fe}_4(\mu_3\text{-S})_4]^{2+,+}$ cores.¹ The first examples of such

higher nuclearity clusters in this field were $[\text{Fe}_6\text{S}_6(\text{SR})_2]^{4-,2-5}$ containing the rather complicated $[\text{Fe}_6(\mu_4\text{-S})(\mu_3\text{-S})_2(\mu_2\text{-S})_6]^{2-}$ core

(1) Berg, J. M.; Holm, R. H. In *Metal Ions in Biology*; Spiro, T. G., Ed.; Interscience: New York, 1982; Vol. 4, Chapter 1.

of idealized C_{2v} symmetry. The isostructural selenium analogues $[\text{Fe}_6\text{Se}_6(\text{SR})_2]^{4-}$ have also been prepared.^{6,7} The remaining members of the set are the prismane clusters $[\text{Fe}_6\text{S}_6\text{L}_6]^{2-3-}$ (L = halide, ArO^-) with the D_{3d} $[\text{Fe}_6(\mu_3\text{-S})_6]^{4+,3+}$ cores,⁸⁻¹¹ the stellated octahedra $[\text{Fe}_6(\mu_3\text{-S})_6(\text{PEt}_3)_6]^{2+,12}$ and a single example, $[\text{Fe}_8\text{S}_6\text{I}_8]^{3-}$,¹³ of a cluster of *anti*- M_6X_8 type, in that the positions of Fe and S atoms are reversed compared to those in the latter cluster. In this case, the core unit is $[\text{Fe}_8(\mu_4\text{-S})_6]^{5+}$.

Experience in this laboratory¹ has indicated that nonaqueous reaction systems containing an iron(II) or iron(III) salt, sulfur or sulfide, and halide and/or thiolate as a terminal ligand do not assemble clusters larger than the Fe_6S_9 type, and most usually afford Fe_4S_4 clusters. Recent results from other laboratories are consistent with these observations.^{11b,14-16} The largest Fe-S cluster assembled in an aqueous system is $[\text{Fe}_4\text{S}_4(\text{SR})_4]^{2-}$.¹⁷ We seek higher nuclearity clusters in order to discern as many structural types as possible, some of which may be eventually identified in metallobiomolecules, and to provide building blocks for the incorporation of vanadium and molybdenum atoms as part of our synthetic approach to the cofactors of nitrogenase. Molybdenum(0) and tungsten(0) tricarbonyl fragments have been integrated in prismane cores by reactions of this type.¹⁸ Noting that all previous Fe-S clusters are charged, we surmised that reaction systems conducted in an essentially nonpolar medium in the presence of *neutral* terminal ligands such as tertiary phosphines might generate larger (or at least different), presumably neutral, clusters. This view receives support from the results of Fenske and co-workers,¹⁹ who have demonstrated the formation of cobalt and nickel sulfide or selenide clusters with nuclearities of six to nine (and even one cluster containing the $\text{Ni}_{13}\text{Se}_{22}$ core!) from the reactions of $\text{M}(\text{PPh}_3)_2\text{Cl}_2$ and $(\text{Me}_3\text{Si})_2\text{S}$ in THF or $(\text{Me}_3\text{Si})_2\text{Se}$ in toluene.

Our first synthetic experiments in nonpolar solvents led to the formation of the neutral septanuclear cluster $\text{Fe}_7\text{S}_6(\text{PET}_3)_4\text{Cl}_3$, whose $[\text{Fe}_7(\mu_4\text{-S})_4(\mu_3\text{-S})_3]^{3+}$ core has the configuration of a monocapped prismane.²⁰ This compound was found to be unstable in solution, slowly converting to a new paramagnetic cluster. In the present work we have synthesized and structurally identified this cluster. As will be shown here, the core conversion that leads to the formation of the latter from $\text{Fe}_7\text{S}_6(\text{PET}_3)_4\text{Cl}_3$ is but one of a number of irreversible transformations that interconnect Fe-S clusters of different nuclearities and core structures. Certain initial results of this work have been reported;²¹ full details are provided here.

Experimental Section

Preparation of Compounds. The compounds $\text{Fe}(\text{PET}_3)_2\text{Cl}_2$,²² $(n\text{-Bu}_4\text{N})_2[\text{Fe}_4\text{S}_4\text{Cl}_4]$,²³ $(n\text{-Bu}_4\text{N})_2[\text{Fe}_4\text{S}_4\text{Br}_4]$,²³ $\text{Fe}_3\text{S}_4(\text{PET}_3)_4\text{Cl}_3$,²⁰ $(n\text{-Bu}_4\text{N})_2[\text{Fe}_4\text{S}_4(\text{SPh})_4]$,²⁴ $(\text{Et}_4\text{N})_3[\text{Fe}_6\text{S}_6\text{Cl}_6]$,⁸ and $(\text{Et}_4\text{N})_3[\text{Fe}_6\text{S}_6\text{Br}_6]$ ⁸ were prepared as previously described. All operations were carried out under a pure dinitrogen atmosphere by using standard Schlenk techniques. THF was distilled from Na/benzophenone, acetonitrile from CaH_2 , and acetone from CaSO_4 . Solvents were degassed immediately prior to use. Anhydrous iron salts (Cerac) and hexamethyldisilthiane (Aldrich, Petrarch) were commercial samples; triethylphosphine was donated by the Cyanamid Corp. and was purified by distillation. Iron analyses were performed by atomic absorption spectrophotometry; other elements were analyzed commercially.

$\text{Fe}(\text{PET}_3)_2\text{Br}_2$. This compound was prepared in a manner analogous to that for $\text{Fe}(\text{PET}_3)_2\text{Cl}_2$. It was obtained as a pale yellow, highly air-sensitive crystalline solid; its identity was confirmed by a crystal structure determination.

$(n\text{-Bu}_4\text{N})_2[\text{Fe}_4\text{Se}_4\text{Cl}_4]$. A suspension of 5.0 g (3.4 mmol) of $(n\text{-Bu}_4\text{N})_4[\text{Fe}_4\text{Se}_4(\text{SPh})_4]$ in 50 mL of acetonitrile was treated with 4.8 mL (41 mmol) of benzoyl chloride. During a 2-h reaction period the solution color changed from deep red-brown to purplish black. Ether was added to the filtrate of the reaction mixture, and the solution was maintained at -20°C overnight. The product was isolated by filtration, washed with ether, and dried in vacuo to yield 3.17 g (80%) of black crystalline solid. Absorption spectrum (acetonitrile; λ_{max} , nm (ϵ_{M})): 310 sh (12 200), 540 (1960), 735 (1440). This spectrum is analogous to that of $[\text{Fe}_4\text{S}_4\text{Cl}_4]^{2-23}$ but with the red shifts of visible bands, a characteristic feature of clusters with the $[\text{Fe}_4\text{Se}_4]^{2+}$ core.²⁵ The cubane structure of this cluster has been further confirmed by an X-ray diffraction study of its Et_4N^+ salt.²⁶

$\text{Fe}_6\text{S}_6(\text{PET}_3)_4\text{Cl}_3$. Method A. A solution of 2.0 g (5.5 mmol) of $\text{Fe}(\text{PET}_3)_2\text{Cl}_2$ in 80 mL of THF was treated with 0.97 mL (5.5 mmol) of $(\text{Me}_3\text{Si})_2\text{S}$ or 0.25 g (5.5 mmol) of Li_2S . The reaction mixture rapidly darkened to deep brown and was stirred for 12-16 h. The filtrate of the reaction mixture was reduced in vacuo to a black, oily residue. This was washed consecutively with hexanes, ether, and acetonitrile until colorless washes were obtained. The dark solid was recrystallized from $\text{CH}_2\text{Cl}_2/\text{hexanes}$ to afford 0.61 g (62%) or 0.54 g (54%) of pure product as a black crystalline solid. $^1\text{H NMR}$ (CDCl_3 ; δ): -7.72 (2), -6.59 (2), -0.15 (3), 0.14 (3). Absorption spectrum (CH_2Cl_2 ; λ_{max} , nm (ϵ_{M})): 320 sh (27 300). Anal. Calcd for $\text{C}_{24}\text{H}_{60}\text{Cl}_2\text{Fe}_6\text{P}_4\text{S}_6$: C, 26.90; H, 5.65; Cl, 6.62; Fe, 31.29; P, 11.57; S, 17.97. Found: C, 26.49; H, 5.67; Cl, 6.61; Fe, 31.01; P, 11.71; S, 18.11.

Method B. A mixture of 0.74 g (2.0 mmol) of $\text{Fe}(\text{PET}_3)_2\text{Cl}_2$ and 0.87 g (1.0 mmol) of $(n\text{-Bu}_4\text{N})_2[\text{Fe}_4\text{S}_4\text{Cl}_4]$ or 1.13 g (1.0 mmol) of $(\text{Et}_4\text{N})_3[\text{Fe}_6\text{S}_6\text{Cl}_6]$ was suspended in 20 mL of acetonitrile and stirred for about 6 h. The black solid isolated by filtration was recrystallized from $\text{CH}_2\text{Cl}_2/\text{hexanes}$ to yield the pure product as 0.51 g (70%) or 0.75 g (70%) of black crystals, identical in all respects with the product of method A.

$\text{Fe}_6\text{S}_6(\text{PET}_3)_4\text{Br}_2$. Method A. A solution of 2.0 g (4.4 mmol) of $\text{Fe}(\text{PET}_3)_2\text{Br}_2$ in 100 mL of THF was treated with 0.78 mL (4.4 mmol) of $(\text{Me}_3\text{Si})_2\text{S}$. The reaction mixture darkened over several minutes. It was refluxed for 24 h, volatiles were removed in vacuo, and the residue was washed consecutively with hexanes, ether, and acetonitrile until the washings were colorless. This material was recrystallized from THF/

- (2) (a) Christou, G.; Holm, R. H.; Sabat, M.; Ibers, J. A. *J. Am. Chem. Soc.* **1981**, *103*, 6269. (b) Christou, G.; Sabat, M.; Ibers, J. A.; Holm, R. H. *Inorg. Chem.* **1982**, *21*, 3518.
- (3) Hagen, K. S.; Watson, A. D.; Holm, R. H. *J. Am. Chem. Soc.* **1983**, *105*, 3905.
- (4) (a) Henkel, G.; Strasdeit, H.; Krebs, B. *Angew. Chem., Int. Ed. Engl.* **1982**, *21*, 201. (b) Strasdeit, H.; Krebs, B.; Henkel, G. *Inorg. Chem.* **1984**, *23*, 1816.
- (5) Zhang, Z.; Liu, X.; Fan, Y. *Kexue Tongbao* **1985**, *30*, 1351.
- (6) Holm, R. H.; Hagen, K. S.; Watson, A. D. In *Chemistry for the Future*; Grünwald, H., Ed.; Pergamon: Oxford, England, 1984; pp 115-124.
- (7) Strasdeit, H.; Krebs, B.; Henkel, G. *Z. Naturforsch., B: Anorg. Chem., Org. Chem.* **1987**, *42B*, 565.
- (8) (a) Kanatzidis, M. G.; Dunham, W. R.; Hagen, W. R.; Coucouvanis, D. *J. Chem. Soc., Chem. Commun.* **1984**, 356. (b) Kanatzidis, M. G.; Hagen, W. R.; Dunham, W. R.; Lester, R. K.; Coucouvanis, D. *J. Am. Chem. Soc.* **1985**, *107*, 953.
- (9) Coucouvanis, D.; Kanatzidis, M. G.; Dunham, W. R.; Hagen, W. R. *J. Am. Chem. Soc.* **1984**, *106*, 7998.
- (10) Kanatzidis, M. G.; Salifoglou, A.; Coucouvanis, D. *J. Am. Chem. Soc.* **1985**, *3358*; *Inorg. Chem.* **1986**, *25*, 2460.
- (11) (a) Saak, W.; Henkel, G.; Pohl, S. *Angew. Chem., Int. Ed. Engl.* **1984**, *23*, 150. (b) Saak, W.; Pohl, S. *Z. Naturforsch., B: Anorg. Chem., Org. Chem.* **1985**, *40B*, 1105.
- (12) (a) Ceconi, F.; Ghilardi, C. A.; Midollini, S. *J. Chem. Soc., Chem. Commun.* **1981**, 640. (b) Agresti, A.; Bacci, M.; Ceconi, F.; Ghilardi, C. A.; Midollini, S. *Inorg. Chem.* **1985**, *24*, 689. (c) Ceconi, F.; Ghilardi, C. A.; Midollini, S.; Orlandini, A. *J. Chem. Soc., Dalton Trans.* **1987**, 831.
- (13) Pohl, S.; Saak, W. *Angew. Chem., Int. Ed. Engl.* **1984**, *23*, 907.
- (14) Cleland, W. E., Jr.; Averill, B. A. *Inorg. Chem.* **1984**, *23*, 4192.
- (15) (a) Müller, A.; Schladerbeck, N. *Chimia* **1985**, *39*, 23. (b) Müller, A.; Schladerbeck, N.; Bögge, H. *Chimia* **1985**, *39*, 24.
- (16) Han, S.; Czernuszewicz, R. S.; Spiro, T. G. *Inorg. Chem.* **1986**, *25*, 2276.
- (17) (a) Kurtz, D. M., Jr.; Stevens, W. C. *J. Am. Chem. Soc.* **1984**, *106*, 1523. (b) Bonomi, F.; Werth, M. T.; Kurtz, D. M., Jr. *Inorg. Chem.* **1985**, *24*, 4331.
- (18) (a) Coucouvanis, D.; Kanatzidis, M. G. *J. Am. Chem. Soc.* **1985**, *107*, 5005. (b) Salifoglou, A.; Kanatzidis, M. G.; Coucouvanis, D. *J. Chem. Soc., Chem. Commun.* **1986**, 559. (c) Kanatzidis, M. G.; Coucouvanis, D. *J. Am. Chem. Soc.* **1986**, *108*, 337. (d) Coucouvanis, D.; Salifoglou, A.; Kanatzidis, M. G.; Simopoulos, A.; Kostikas, A. *J. Am. Chem. Soc.* **1987**, *109*, 3807.
- (19) (a) Fenske, D.; Hachgenei, J.; Ohmer, J. *Angew. Chem., Int. Ed. Engl.* **1985**, *24*, 706. (b) Fenske, D.; Ohmer, J.; Hachgenei, J. *Angew. Chem., Int. Ed. Engl.* **1985**, *24*, 993. (c) Fenske, D.; Ohmer, J. *Angew. Chem., Int. Ed. Engl.* **1987**, *26*, 148.

- (20) Noda, I.; Snyder, B. S.; Holm, R. H. *Inorg. Chem.* **1986**, *25*, 3851.
- (21) Snyder, B. S.; Reynolds, M. S.; Noda, I.; Holm, R. H. *Inorg. Chem.* **1988**, *27*, 595.
- (22) Booth, G.; Chatt, J. *J. Chem. Soc.* **1962**, 2009.
- (23) Wong, G. B.; Bobrik, M. A.; Holm, R. H. *Inorg. Chem.* **1978**, *17*, 578.
- (24) Christou, G.; Ridge, B.; Rydon, H. N. *J. Chem. Soc., Dalton Trans.* **1978**, 1423.
- (25) Bobrik, M. A.; Laskowski, E. J.; Johnson, R. W.; Gillum, W. O.; Berg, J. M.; Hodgson, K. O.; Holm, R. H. *Inorg. Chem.* **1978**, *17*, 1402.
- (26) Cen, W.; Lin, H. *Jiegou Huaxue* **1986**, *5*, 203.

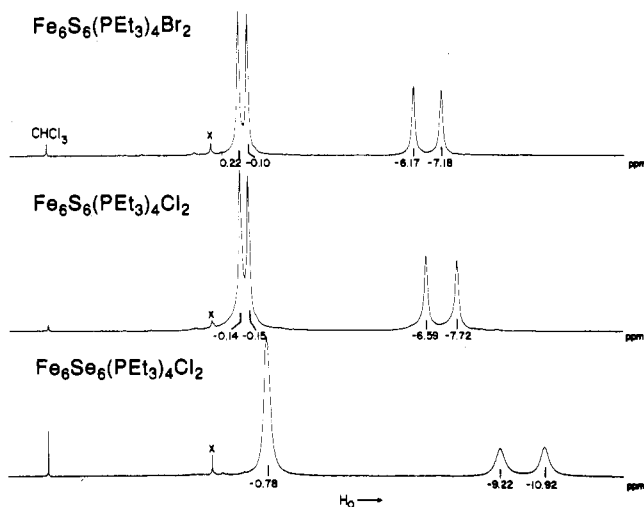


Figure 1. ^1H NMR spectra of $\text{Fe}_6\text{S}_6(\text{PEt}_3)_4\text{Br}_2$, $\text{Fe}_6\text{S}_6(\text{PEt}_3)_4\text{Cl}_2$, and $\text{Fe}_6\text{Se}_6(\text{PEt}_3)_4\text{Cl}_2$ in CDCl_3 solutions at $\sim 25^\circ\text{C}$. Chemical shifts are indicated.

hexanes to afford 0.14 g (16%) of pure product as a black crystalline solid. ^1H NMR (CDCl_3 ; δ): -7.18 (2), -6.17 (2), -0.10 (3), 0.22 (3). Absorption spectrum (CH_2Cl_2 ; λ_{max} , nm (ϵ_{M}): 310 sh (33 200). Anal. Calcd for $\text{C}_{24}\text{H}_{60}\text{Br}_2\text{Fe}_6\text{P}_4\text{S}_6$: C, 24.83; H, 5.21; Br, 13.78; Fe, 28.89; P, 10.68; S, 16.59. Found: C, 24.76; H, 5.30; Br, 13.84; Fe, 28.49; P, 10.77; S, 16.46.

Method B. Use of the procedure above with 3.0 mmol of $\text{Fe}(\text{PEt}_3)_2\text{Br}_2$ and 1.5 mmol of $(\text{Et}_4\text{N})_2[\text{Fe}_4\text{S}_4\text{Br}_4]$ or $(\text{Et}_4\text{N})_3[\text{Fe}_6\text{S}_6\text{Br}_6]$ gave the product as a black crystalline solid (57% or 65%), identical in all respects with the product of method A.

$\text{Fe}_6\text{Se}_6(\text{PEt}_3)_4\text{Cl}_2$. Method A. A suspension of 0.50 g (5.3 mmol) of $\text{Li}_2\text{Se}^{27}$ in 25 mL of toluene was treated dropwise with a solution of 1.26 mL (10.6 mmol) of Me_3SiCl in 20 mL of toluene. After it was stirred overnight, this solution of $(\text{Me}_3\text{Si})_2\text{Se}^{28}$ was filtered into a solution of 2.0 g (5.5 mmol) of $\text{Fe}(\text{PEt}_3)_2\text{Cl}_2$ in 30 mL of toluene. After being stirred for 16 h, the reaction mixture was filtered and solvent was removed in vacuo from the filtrate. The residue was washed consecutively with hexanes, ether, and acetonitrile until the washings were colorless. The residue was recrystallized from CH_2Cl_2 /hexanes to yield 0.12 g (10%) of pure product as a black crystalline solid. ^1H NMR (CDCl_3 ; δ): -10.92 (2), -9.22 (2), -0.78 (6). Absorption spectrum (CH_2Cl_2): featureless to 280 nm. Anal. Calcd for $\text{C}_{24}\text{H}_{60}\text{Cl}_2\text{Fe}_6\text{P}_4\text{Se}_6$: C, 21.30; H, 4.47; Cl, 5.24; Fe, 24.78; P, 9.16; Se, 35.04. Found: C, 21.86; H, 4.58; Cl, 5.34; Fe, 24.56; P, 9.17; Se, 34.88.

Method B. Use of the procedure above with 1.72 mmol of $\text{Fe}(\text{PEt}_3)_2\text{Cl}_2$ and 0.86 mmol of $(n\text{-Bu}_4\text{N})_2[\text{Fe}_4\text{Se}_4\text{Cl}_4]$ gave the product as a black crystalline solid (84%) identical in all respects with the product of method A.

In addition to the above, $\text{Fe}_6\text{S}_6(\text{PEt}_3)_4\text{I}_2$ was prepared as a black crystalline solid by methods A and B in 14% and 65% yields, respectively. ^1H NMR (CDCl_3 ; δ): -6.36 (2), -5.57 (2), -0.10 (3), 0.30 (3). $\text{Fe}_6\text{S}_6(\text{PMe}_3)_4\text{Cl}_2$ was obtained by method A in 60% yield as a black crystalline solid. ^1H NMR (CDCl_3 ; δ): -12.76 (1), -11.89 (1). $\text{Fe}_6\text{S}_6(\text{P-}n\text{-Bu}_3)_4\text{Cl}_2$ was also obtained by method A in unoptimized yield, as an extremely soluble black crystalline solid used for an x-ray structural determination. ^1H NMR (CDCl_3 ; δ): -8.31 (2), -7.07 (2), 1.0 (m, 7). These compounds were pure by the NMR criterion and were not analyzed.

Core Conversion Reactions. (a) $\text{Fe}_7\text{S}_6(\text{PEt}_3)_4\text{Cl}_3$ to $\text{Fe}_6\text{S}_6(\text{PEt}_3)_4\text{Cl}_2$. Aliquots were removed from a 5.6 mM solution of $\text{Fe}_7\text{S}_6(\text{PEt}_3)_4\text{Cl}_3$ in CDCl_3 at ca. 2-h intervals and were filtered to remove a slight amount of a dark insoluble material that formed during the reaction. The course of the reaction was monitored by means of the ^1H NMR spectra of the filtrates. The product was identified by its characteristic spectrum, shown in Figure 1, and was quantitated by signal integration vs residual CHCl_3 . A 95% conversion was found after 22 h.

For the following reactions, yields are given in terms of g-atoms of Fe.

(b) $\text{Fe}_6\text{S}_6(\text{PEt}_3)_4\text{Cl}_2$ to $[\text{Fe}_4\text{S}_4\text{Cl}_4]^{2-}$, $[\text{Fe}_6\text{S}_6\text{Cl}_6]^{2-}$, and $[\text{Fe}_2\text{S}_2]^{2-}$. A suspension of 0.25 g (0.23 mmol) of $\text{Fe}_6\text{S}_6(\text{PEt}_3)_4\text{Cl}_2$, 0.075 g (2.3 mmol) of sulfur, and 0.54 g (0.93 mmol) of $(\text{PPN})\text{Cl}$ ($\text{PPN} = [(\text{Ph}_3\text{P})_2\text{N}]^+$) in 20 mL of acetone was stirred overnight. The brown solid was separated

by filtration. Examination of the red-brown filtrate by ^{31}P NMR revealed 3.7 equiv of Et_3PS (δ 53.4), after integration against an internal standard of this compound, and a slight amount of Et_3PO (δ 20.2). From the absorption spectrum, assuming the same extinction coefficient of the 690-nm band as in acetonitrile, 23 $[\text{Fe}_4\text{S}_4\text{Cl}_4]^{2-}$ was formed in 30% yield. The solid product was washed with a 20-mL portion of acetone and treated with acetonitrile. The solution was filtered, ether was added to the filtrate, and the solution was maintained overnight at -20°C . Filtration afforded 0.20 g of a black crystalline solid that showed no isotropically shifted ^1H NMR signals and had a featureless UV/visible absorption spectrum. The material was identified by X-ray structural analysis as $(\text{PPN})_3[\text{Fe}_6\text{S}_6\text{Cl}_6]$ (49%). The residue that remained from the acetonitrile treatment was taken up in DMF, and unreacted sulfur was removed by filtration. Addition of ether to the filtrate and maintenance overnight at -20°C gave 0.060 g of a dark brown crystalline solid, which was shown to be $(\text{PPN})_2[\text{Fe}_2\text{S}_2]$ (6%) from its absorption spectrum. 29 When $\text{Ph}_4\text{P}\text{Cl}$ was utilized in the foregoing procedure, $(\text{Ph}_4\text{P})_2[\text{Fe}_2\text{S}_2]$ (8%) was obtained. This compound was identified from its unit cell dimensions, which were identical with those reported earlier, 29 and a structure solution further confirmed the presence of $[\text{Fe}_2\text{S}_2(\text{S}_2)]^{2-}$.

(c) $\text{Fe}_6\text{S}_6(\text{PEt}_3)_4\text{Cl}_2$ to $[\text{Fe}_4\text{S}_4\text{Cl}_4]^{2-}$. A suspension of 0.25 g (0.23 mmol) of $\text{Fe}_6\text{S}_6(\text{PEt}_3)_4\text{Cl}_2$, 0.10 g (0.92 mmol) of $(\text{Me}_4\text{N})\text{Cl}$, and 0.075 g (2.3 mmol) of sulfur in 25 mL of acetone was stirred overnight. Ether (25 mL) was added to the reaction mixture filtrate, and the mixture was stored at -20°C overnight. A black crystalline solid was collected and washed with ether, giving 0.10 g of material. This was identified as $(\text{Me}_4\text{N})_2[\text{Fe}_4\text{S}_4\text{Cl}_4]$ (46%) from the absence of isotropically shifted ^1H NMR resonances and its UV/visible absorption spectrum. 23 Formation of 4.1 equiv of Et_3PS was established from the ^{31}P NMR spectrum of the filtrate.

(d) $\text{Fe}_6\text{S}_6(\text{PEt}_3)_4\text{Cl}_2$ to $[\text{Fe}_4\text{S}_4(\text{S-}p\text{-tol})_4]^{2-}$. A suspension of 1.0 g (0.93 mmol) of $\text{Fe}_6\text{S}_6(\text{PEt}_3)_4\text{Cl}_2$, 1.08 g (5.58 mmol) of $(\text{Me}_4\text{N})(\text{S-}p\text{-tol})$ ($\text{tol} = \text{tolyl}$), and 0.18 g (5.58 mmol) of sulfur in 50 mL of acetonitrile rapidly turned deep red-brown, and stirring was continued overnight. An intractable black solid was separated by filtration. Ether was added to the dark red-brown filtrate, and the solution was stored overnight at -20°C . Filtration afforded 0.24 g of a black crystalline solid identified as $(\text{Me}_4\text{N})_2[\text{Fe}_4\text{S}_4(\text{S-}p\text{-tol})_4]$ (17%) from its UV/visible 30 and ^1H NMR 31 spectra.

Collection and Reduction of X-ray Data. Single crystals of $\text{Fe}_6\text{S}_6(\text{PEt}_3)_4\text{X}_2$ ($\text{X} = \text{Cl}, \text{Br}$) were grown by ether diffusion into CH_2Cl_2 solutions. Examination of multiple preparations of these crystals indicated that they possess tetragonal symmetry. Precession photographs confirmed the observed cell constants and were indicative of the $4/mmm$ Laue class. Systematic extinctions were inconsistent with any space group in this class but, rather, indicated space group $P4_2/n$ (Laue class $4/m$). In the absence of any evidence for physical twinning, we concluded that these crystals are twins of merohedry and turned attention to crystals more amenable to structure solution. Crystals of $\text{Fe}_6\text{S}_6(\text{P-}n\text{-Bu}_3)_4\text{Cl}_2$ were obtained by vapor diffusion of acetonitrile into a THF solution. $\text{Fe}(\text{PEt}_3)_2\text{Br}_2$ and $(\text{PPN})_3[\text{Fe}_6\text{S}_6\text{Cl}_6]$ were crystallized by slow cooling of an ether solution and ether diffusion into an acetonitrile solution, respectively. A black needle of $\text{Fe}_6\text{S}_6(\text{P-}n\text{-Bu}_3)_4\text{Cl}_2$, a pale yellow block of $\text{Fe}(\text{PEt}_3)_2\text{Br}_2$, and a black irregularly shaped crystal of $(\text{PPN})_3[\text{Fe}_6\text{S}_6\text{Cl}_6]$ were mounted in glass capillaries under a dinitrogen atmosphere. Data collection was carried out at ambient temperature on a Nicolet P3F diffractometer, equipped with a graphite monochromator. Data collection parameters are provided in Table I. Unit cell parameters were obtained from 25 machine-centered reflections ($20^\circ \leq 2\theta \leq 25^\circ$). Intensities of three check reflections monitored every 123 reflections revealed no significant decay over the course of data collection. Data sets were processed with the program XTAPE of the SHELXTL program package (Nicolet XRD Corp., Madison, WI), and an empirical absorption correction was applied to the last two compounds with use of the program PSCOR. For $\text{Fe}_6\text{S}_6(\text{P-}n\text{-Bu}_3)_4\text{Cl}_2$, axial photographs indicated Laue class $4/m$ and the systematic absences hkl ($h + k + l = 2n + 1$), $hk0$ ($h + k = 2n + 1$), $0kl$ ($k + l = 2n + 1$), hhl ($l = 2n + 1$), $0k0$ ($k = 2n + 1$), and $00l$ ($l \neq 4n$) are consistent with the space group $I4_1$. For $\text{Fe}(\text{PEt}_3)_2\text{Br}_2$, axial photographs and the systematic absences $h0l$ ($h + l = 2n + 1$), $h00$ ($h = 2n + 1$), and $00l$ ($l = 2n + 1$) are consistent with the space groups Pn and $P2/n$. Simple E statistics indicated the noncentrosymmetric space group as the correct choice. For $(\text{PPN})_3[\text{Fe}_6\text{S}_6\text{Cl}_6]$, axial photographs and the systematic absences hkl ($h + k = 2n + 1$), $h0l$

(29) Coucouvanis, D.; Swenson, D.; Stremple, P.; Baenziger, N. C. *J. Am. Chem. Soc.* **1979**, *101*, 3392.

(30) DePamphilis, B. V.; Averill, B. A.; Herskovitz, T.; Que, L., Jr.; Holm, R. H. *J. Am. Chem. Soc.* **1974**, *96*, 4159.

(31) Holm, R. H.; Phillips, W. D.; Averill, B. A.; Mayerle, J. J.; Herskovitz, T. *J. Am. Chem. Soc.* **1974**, *96*, 2109.

(27) Drake, J. E.; Galvincevski, B. M. *Inorg. Synth.* **1980**, *20*, 171.

(28) Schmidt, M.; Ruf, H. Z. *Anorg. Allg. Chem.* **1963**, *321*, 270.

Table I. Summary of Crystal Data, Intensity Collection, and Refinement Parameters for Fe(PEt₃)₂Br₂, Fe₆S₆(P-*n*-Bu₃)₄Cl₂, and (PPN)₃[Fe₆S₆Cl₆]

	Fe(PEt ₃) ₂ Br ₂	Fe ₆ S ₆ (P- <i>n</i> -Bu ₃) ₄ Cl ₂	(PPN) ₃ [Fe ₆ S ₆ Cl ₆]
formula	C ₁₂ H ₃₀ Br ₂ FeP ₂	C ₄₈ H ₁₀₈ Cl ₂ Fe ₆ P ₄ S ₆	C ₁₀₈ H ₉₀ Cl ₆ Fe ₆ N ₃ P ₆ S ₆
mol wt	451.83	1407.09	2353.8
<i>a</i> , Å	7.316 (1)	33.78 (1)	28.929 (8)
<i>b</i> , Å	12.316 (2)		15.296 (5)
<i>c</i> , Å	11.356 (2)	12.362 (7)	28.898 (6)
β, deg	97.15 (2)		122.39 (2)
cryst syst	monoclinic	tetragonal	monoclinic
<i>V</i> , Å ³	1015 (1)	14 108 (9)	10 797 (5)
<i>Z</i>	2	8	4
<i>d</i> _{calcd} (<i>d</i> _{obsd}), g/cm ³	1.48 ^a	1.32 (1.31) ^b	1.45 (1.43) ^c
space group	<i>Pn</i>	<i>I</i> ₄	<i>C2/c</i>
cryst dimens, mm	0.40 × 0.40 × 0.45	0.20 × 0.20 × 0.50	0.50 × 0.50 × 0.50
radiation	Mo Kα (λ = 0.710 69 Å)	Mo Kα (λ = 0.710 69 Å)	Mo Kα (λ = 0.710 69 Å)
abs coeff, μ, cm ⁻¹	95.6	15.8	11.8
scan speed, deg/min	2.0–29.3 (θ–2θ scan)	2.0–29.3 (ω scan)	2.0–29.3 (ω scan)
scan range, deg	0.8 below Kα ₁ to 0.8 above Kα ₂	0.7 below Kα ₁ to 0.7 above Kα ₂	0.7 below Kα ₁ to 0.7 above Kα ₂
bkgd/scan time ratio	0.25	0.25	0.50
data collectn limits, deg	3 ≤ 2θ ≤ 50	3 ≤ 2θ ≤ 45	3 ≤ 2θ ≤ 50
no. of data collected	2376 (+ <i>h</i> , + <i>k</i> , ± <i>l</i>)	4687 (+ <i>h</i> , + <i>k</i> , ± <i>l</i>)	11 657 (+ <i>h</i> , + <i>k</i> , ± <i>l</i>)
<i>R</i> _{merge} , % ^d	5.51	3.38	2.36
no. of unique data	1205 (<i>F</i> _o ² > 3σ(<i>F</i> _o ²))	2396 (<i>F</i> _o ² > 1.8σ(<i>F</i> _o ²))	5129 (<i>F</i> _o ² > 3.0σ(<i>F</i> _o ²))
no. of variables	151	352	609
<i>R</i> (<i>R</i> _w), %	4.66 (5.32) ^f	9.50 (7.65) ^g	6.06 (10.98) ^h

^a Density measurements by neutral buoyancy were unobtainable owing to the high solubility of the crystals in most organic solvents and their instability in inorganic solvents. ^b Determined by neutral buoyancy in CCl₄/acetonitrile. ^c Determined by neutral buoyancy in CCl₄/hexane. ^d *R*_{merge} = [Σ_{*i*} |*N_i*(Σ(*F_i* - *F_j*)) / Σ_{*j*} |*N_j*(Σ(*F_j*))], where *N_i* is the number of equivalent reflections merged to give the mean, *F_i*, *F_j* is any one member of this set, and the calculations are done on *F_o*². ^e *R* = Σ||*F_o* - |*F_c*|| / Σ|*F_o*|; *R*_w = [Σw(|*F_o*|² - |*F_c*|²) / Σw|*F_o*|²]^{1/2}. ^f Weighting scheme for least-squares refinement follows a three-term Chebyshev polynomial (75.52, 104.52, 36.08). Caruthers, J. R. *Acta Crystallogr., Sect. A: Cryst. Phys., Diffraction, Theor. Gen. Crystallogr.* **1975**, *A35*, 698. ^g Weighting scheme for least-squares refinement: *w* = (1/σ(*F_o*))². ^h Weighting scheme for least-squares refinement: *P*(1) = *F*(min(|*F_o*|² - |*F_c*|²)) = 14.0, *w* = (*F_o*/*P*(1))², *F_o* ≤ *P*(1); (*P*(1)/*F_o*)², *F_o* > *P*(1).

(*h*, *l* = 2*n* + 1), 0*kl* (*k* = 2*n* + 1), *hk0* (*h* + *k* = 2*n* + 1), 0*k0* (*k* = 2*n* + 1), *h00* (*h* = 2*n* + 1), and 00*l* (*l* = 2*n* + 1) are consistent with the space groups *Cc* and *C2/c*. Simple *E* statistics indicated the centrosymmetric space groups as the correct choice. Subsequent structure solutions and refinements corroborated the choices of space groups of the three compounds.

Structure Solution and Refinement. Atomic scattering factors were taken from a standard source.³² All heavy atoms in Fe₆S₆(P-*n*-Bu₃)₄Cl₂ and Fe(PEt₃)₂Br₂ and all atoms in the anion of (PPN)₃[Fe₆S₆Cl₆] were located by direct methods with MULTAN. All carbon atoms were located in successive Fourier maps and were refined by using CRYSTALS. The organic groups of Fe₆S₆(P-*n*-Bu₃)₄Cl₂ were found to be disordered. A final difference Fourier map revealed 10 peaks in the range of 0.5–0.8 e/Å³ that were located within bonding distance of the *n*-butyl groups. The disorder was not treated due to limitations in the number of data. This also required that the carbons be treated isotropically and that C–C distances and C–C–C angles be constrained to their normal values. The above treatment resulted in rather large thermal parameters for the disordered atoms. However, small standard deviations on the positional parameters for the core atoms suggest that the heavy-atom portion of the structure is well-defined. Isotropic refinement converged at conventional *R* values of 12.8% (Fe₆S₆(P-*n*-Bu₃)₄Cl₂), 10.4% (Fe(PEt₃)₂Br₂), and 13.9% ((PPN)₃[Fe₆S₆Cl₆]). All non-carbon atoms in Fe₆S₆(P-*n*-Bu₃)₄Cl₂ and all non-hydrogen atoms in the other two structures were described anisotropically. In the last two cases hydrogen atoms were included at 0.95 Å from, and with 1.2× the isotropic thermal parameter of, the bonded carbon atom. Final *R* values are given in Table I, and atom positional parameters for Fe(PEt₃)₂Br₂ and Fe₆S₆(P-*n*-Bu₃)₄Cl₂ are listed in Tables II and III; those for (PPN)₃[Fe₆S₆Cl₆] have been deposited as supplementary material.³³

Other Physical Measurements. All measurements were performed under strictly anaerobic conditions. Absorption spectra were determined on a Cary 219 spectrophotometer. ¹H and ³¹P NMR spectra were recorded on Bruker AM 250 and WM 300 spectrometers, respectively, with internal Me₄Si and external aqueous phosphoric acid neutralized to pH 7 as the appropriate references. Electrochemical experiments were carried out with standard PAR instrumentation, by using a glassy-carbon working electrode, a SCE reference electrode, and 0.2 M (*n*-Bu₄N)ClO₄

Table II. Positional Parameters (×10⁴) for Fe(PEt₃)₂Br₂

atom	<i>x/a</i>	<i>y/b</i>	<i>z/c</i>
Fe(1)	4852	2649	-70
Br(1)	6895 (3)	1183 (1)	458 (2)
Br(2)	5921 (3)	4365 (1)	-659 (2)
P(1)	2738 (5)	2025 (3)	-1725 (3)
P(2)	3139 (5)	2952 (3)	1623 (3)
C(11)	1008 (31)	1013 (18)	-1489 (16)
C(12)	1703 (38)	60 (18)	-836 (21)
C(13)	1350 (28)	3128 (15)	-2495 (16)
C(14)	272 (37)	2868 (24)	-3643 (22)
C(15)	3909 (27)	1391 (16)	-2873 (15)
C(16)	5433 (40)	1997 (25)	-3225 (18)
C(21)	892 (20)	3676 (12)	1399 (16)
C(22)	1092 (23)	4748 (13)	796 (14)
C(23)	2582 (21)	1661 (15)	2293 (14)
C(24)	1746 (32)	1703 (21)	3411 (21)
C(25)	4460 (20)	3771 (12)	2769 (13)
C(26)	6364 (24)	3287 (17)	3188 (16)

supporting electrolyte in dichloromethane solutions.

Results and Discussion

Structure of Fe(PEt₃)₂Br₂. For cluster synthesis in a nonpolar medium such as THF, we utilized the soluble complexes Fe(PEt₃)₂X₂ (X = Cl⁻, Br⁻) as reactants. The chloride complex has been previously claimed by Booth and Chatt,²² who described it as unstable and did not characterize it further. While a tetrahedral structure is anticipated from the magnetic moments (4.7–5.3 μ_B) of other Fe(PR₃)₂X₂ complexes,^{22,34,35} the moment of red Fe(PHEt₂)₂Cl₂ (3.61 μ_B³⁵) is inconsistent with this stereochemistry and implies a planar structure if the compound is molecular. To improve the characterization of Fe(PR₃)₂X₂ complexes, for which there are no previous structural data, the crystal structure of Fe(PEt₃)₂Br₂, which readily crystallized from ether as yellow blocks, was determined.

(32) Cromer, D. T.; Waber, J. T. *International Tables for X-Ray Crystallography*; Kynoch: Birmingham, England, 1974.

(33) See the paragraph at the end of this article concerning supplementary material available.

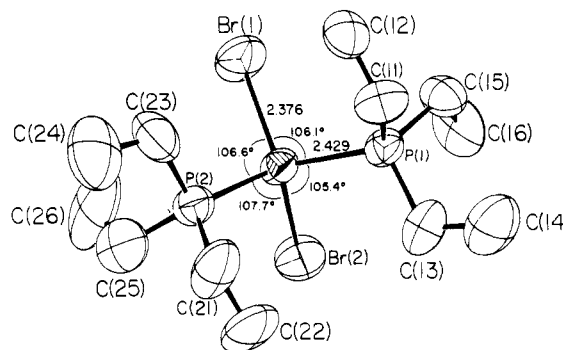
(34) Pignolet, L. H.; Forster, D.; Horrocks, W. D., Jr. *Inorg. Chem.* **1968**, *7*, 828.

(35) Issleib, K.; Döll, G. *Z. Anorg. Allg. Chem.* **1960**, *305*, 1.

Table III. Positional Parameters ($\times 10^4$) for $\text{Fe}_6\text{S}_6(\text{P}-n\text{-Bu}_3)_4\text{Cl}_2$

atom	x/a	y/b	z/c
Fe(1)	2433	299	10722
Fe(2)	2709 (1)	-396 (1)	10007 (6)
Fe(3)	2027 (1)	-146 (1)	9125 (6)
Fe(4)	2708 (1)	221 (1)	8680 (6)
Fe(5)	2047 (1)	636 (1)	9108 (6)
Fe(6)	2037 (2)	-367 (2)	11182 (6)
S(1)	2658 (3)	-190 (3)	11720 (9)
S(2)	3153 (3)	-243 (3)	8829 (10)
S(3)	2162 (3)	-740 (3)	9707 (9)
S(4)	1789 (3)	223 (3)	10444 (8)
S(5)	2161 (3)	221 (3)	7707 (8)
S(6)	2663 (3)	766 (3)	9677 (9)
P(1)	2419 (3)	721 (3)	12172 (10)
P(2)	3080 (3)	-945 (3)	10512 (10)
P(3)	1432 (3)	-350 (3)	8379 (10)
P(4)	3069 (3)	523 (3)	7328 (9)
Cl(1)	1674 (3)	1157 (3)	8774 (11)
Cl(2)	1647 (3)	-641 (3)	12379 (10)
C(1)	2247 (6)	527 (10)	13547 (18)
C(2)	1826 (7)	424 (10)	13479 (19)
C(3)	1688 (9)	268 (13)	14581 (22)
C(4)	1276 (11)	157 (13)	14507 (26)
C(5)	2120 (8)	1189 (8)	11857 (18)
C(6)	2178 (10)	1477 (7)	12737 (27)
C(7)	1855 (10)	1771 (12)	12704 (31)
C(8)	1952 (13)	2068 (11)	11946 (41)
C(9)	2919 (9)	987 (6)	12415 (33)
C(10)	3214 (9)	699 (9)	12640 (41)
C(11)	3606 (10)	888 (13)	12590 (38)
C(12)	3662 (16)	1121 (17)	13542 (52)
C(13)	3483 (8)	-831 (8)	11593 (18)
C(14)	3744 (11)	-559 (11)	11180 (25)
C(15)	4070 (13)	-480 (14)	12019 (30)
C(16)	4359 (17)	-225 (24)	11556 (41)
C(17)	3320 (5)	-1204 (11)	9320 (28)
C(18)	3012 (7)	-1364 (11)	8624 (26)
C(19)	3196 (10)	-1648 (11)	7833 (37)
C(20)	2973 (15)	-1643 (15)	6849 (35)
C(21)	2709 (8)	-1273 (11)	11106 (20)
C(22)	2831 (13)	-1378 (16)	12184 (32)
C(23)	2551 (9)	-1664 (16)	12627 (34)
C(24)	2752 (17)	-1916 (16)	13341 (52)
C(25)	1146 (8)	100 (6)	8116 (18)
C(26)	776 (9)	-8 (8)	7578 (45)
C(27)	605 (13)	352 (13)	7054 (27)
C(28)	427 (13)	594 (11)	7865 (41)
C(29)	1133 (9)	-690 (6)	9300 (29)
C(30)	869 (12)	-459 (7)	9916 (32)
C(31)	537 (10)	-720 (11)	10315 (37)
C(32)	396 (12)	-568 (14)	11327 (37)
C(33)	1532 (10)	-624 (8)	6993 (23)
C(34)	1802 (13)	-922 (15)	7160 (27)
C(35)	1831 (13)	-1162 (10)	6180 (38)
C(36)	2056 (19)	-947 (19)	5378 (39)
C(37)	3296 (6)	114 (11)	6439 (30)
C(38)	2985 (8)	-75 (10)	5827 (36)
C(39)	3159 (13)	-256 (13)	4828 (26)
C(40)	3310 (19)	-637 (15)	5085 (48)
C(41)	3487 (8)	857 (5)	7868 (27)
C(42)	3749 (10)	623 (8)	8529 (29)
C(43)	4131 (9)	842 (12)	8673 (36)
C(44)	4273 (13)	778 (18)	9744 (42)
C(45)	2732 (10)	823 (8)	6500 (25)
C(46)	2739 (13)	1211 (10)	6869 (27)
C(47)	2572 (16)	1475 (10)	6018 (25)
C(48)	2380 (15)	1794 (13)	6517 (37)

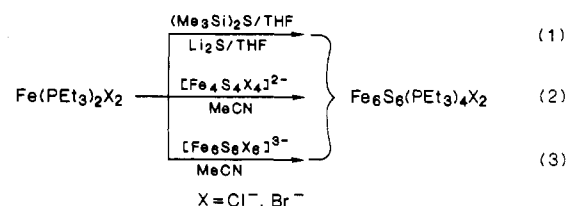
The structure, shown in Figure 2, conforms to distorted-tetrahedral stereochemistry. Selected bond distances and angles are collected in Table IV. The Br–Fe–Br angle of $121.9(1)^\circ$ is enlarged, and the remaining bond angles at iron are slightly compressed, relative to the exact tetrahedral angle. Other dimensions are unexceptional. The foregoing angle is comparable to X–M–X angles in the tetrahedral structures of $\text{Mn}(\text{PET}_3)_2\text{Cl}_2$ ³⁶

**Figure 2.** Structure of $\text{Fe}(\text{PET}_3)_2\text{Br}_2$, showing 50% probability ellipsoids, the atom-labeling scheme, and selected bond angles and mean distances (Å).**Table IV.** Selected Interatomic Distances (Å) and Angles (deg) for $\text{Fe}(\text{PET}_3)_2\text{Br}_2$

Fe(1)–Br(1)	2.373 (2)	Fe(1)–P(1)	2.407 (4)
Fe(1)–Br(2)	2.379 (2)	Fe(1)–P(2)	2.450 (4)
mean	2.376	mean	2.429
Br(1)–Fe(1)–Br(2)	121.9 (1)	Br(1)–Fe(1)–P(1)	106.1 (1)
		Br(2)–Fe(1)–P(1)	105.4 (1)
P(1)–Fe(1)–P(2)	108.6 (1)	Br(1)–Fe(1)–P(2)	106.6 (1)
		Br(2)–Fe(1)–P(2)	107.7 (1)
		mean	106.5

(120.0°) and $\text{Ni}(\text{PPh}_3)_2\text{X}_2$ (Cl ,^{37a} 120.9° ; Br ,^{37b} 126.3°) and larger than those in $\text{Co}(\text{PPh}_3)_2\text{X}_2$ ³⁸ (Cl , 117.3° ; Br , 115.2°), $\text{Cd}(\text{PPh}_3)_2\text{Cl}_2$ ³⁹ (113.9°), $\text{Hg}(\text{PPh}_3)_2\text{X}_2$ (Cl ,^{40a} 110.7° ; I ,^{40b} 110.4°), and $\text{Hg}(\text{PET}_3)_2\text{Cl}_2$ ⁴¹ (105.5°). For these phosphine complexes, there is a tendency for the X–M–X angle to decrease as the Shannon tetrahedral radius⁴² of the metal ion increases, suggesting a progressive alleviation of ligand–ligand repulsion as bond lengths increase.

Preparation of $\text{Fe}_6\text{S}_6(\text{PET}_3)_4\text{X}_2$. $\text{Fe}_6\text{S}_6(\text{PET}_3)_4\text{Cl}_2$ was prepared in THF solution by the reaction of equimolar amounts of $\text{Fe}(\text{PET}_3)_2\text{Cl}_2$ and $(\text{Me}_3\text{Si})_2\text{S}$ or Li_2S in THF (eq 1) and was obtained in 62% or 52% purified yield as an air-sensitive, black crystalline solid, soluble in weakly polar or nonpolar solvents. Several



variations in reactants and solvent were unproductive. Utilization of elemental sulfur instead of a sulfide source afforded only FeCl_2 and Et_3PS . $\text{Fe}(\text{PPh}_3)_2\text{Cl}_2$ ³⁴ and $(\text{Me}_3\text{Si})_2\text{S}$ gave an intractable black solid. $\text{Fe}_6\text{S}_6(\text{PET}_3)_4\text{Cl}_2$ was also obtained in 70% yield by the core expansion reaction 2 involving the cubane cluster $[\text{Fe}_4\text{S}_4\text{Cl}_4]^{2-}$. Additionally, this compound was produced in reaction 3, which results in a one-electron reduction of the prismane cluster $[\text{Fe}_6\text{S}_6\text{Cl}_6]^{3-}$ and attendant core structural change (vide infra). Reaction 2 is the preparative method of choice and has been scaled up by a factor of 10 with no reduction in yield. Use of $\text{Fe}(\text{PET}_3)_2\text{Br}_2$ in reactions 1 (with $(\text{Me}_3\text{Si})_2\text{S}$), 2 (with

(37) (a) Bruins Slot, H. J.; van Havere, W. K. L.; Noordik, J. H.; Beurskens, P. J.; Royo, P. *J. Cryst. Spectrosc. Res.* **1984**, *14*, 623.(38) Carlin, R. L.; Chirico, R. D.; Sinn, E.; Mennenga, G.; de Jongh, L. J. *Inorg. Chem.* **1982**, *21*, 2218.(39) Cameron, A. F.; Forrest, K. P.; Ferguson, G. *J. Chem. Soc. A* **1971**, 1286.(40) (a) Bell, N. A.; Dee, T. D.; Goldstein, M.; McKenna, P. J.; Nowell, I. *Inorg. Chim. Acta* **1983**, *71*, 135. (b) Fäth, L. *Chem. Scr.* **1976**, *9*, 71.(41) Bell, N. A.; Dee, T. D.; Goggin, P. L.; Goldstein, M.; Goodfellow, R. J.; Jones, T.; Kessler, K.; McEwan, D. M. *J. Chem. Res., Miniprint* **1981**, 201.(42) Shannon, R. D. *Acta Crystallogr., Sect. A: Cryst. Phys., Diffraction, Theor. Gen. Crystallogr.* **1976**, *A32*, 751.

Table V. Selected Interatomic Distances (Å) and Angles (deg) for $\text{Fe}_6\text{S}_6(\text{P-}n\text{-Bu}_3)_4\text{Cl}_2$

Fe(1)–Fe(2)	2.678 (5)	Fe(1)–Fe(5)	2.643 (6)	Fe(5)–S(4)	2.331 (10)	Fe(1)–S(4)	2.215 (10)
Fe(3)–Fe(2)	2.684 (7)	Fe(3)–Fe(5)	2.645 (6)	Fe(6)–S(4)	2.345 (10)	Fe(3)–S(4)	2.203 (10)
Fe(1)–Fe(4)	2.702 (6)	Fe(1)–Fe(6)	2.679 (5)	mean	2.338	mean	2.209
Fe(3)–Fe(4)	2.670 (6)	Fe(3)–Fe(6)	2.650 (7)	Fe(1)–P(1)	2.289 (11)	Fe(5)–Cl(1)	2.200 (11)
mean	2.684	mean	2.654	Fe(2)–P(2)	2.324 (11)	Fe(6)–Cl(2)	2.186 (12)
Fe(2)–Fe(6)	2.696 (7)	Fe(1)–Fe(3)	2.835 (6)	Fe(3)–P(3)	2.316 (11)	mean	2.193
Fe(4)–Fe(5)	2.689 (7)	Fe(2)–Fe(4)	2.655 (7)	Fe(4)–P(4)	2.306 (11)		
mean	2.693			mean	2.309		
Fe(1)–S(1)	2.197 (10)	Fe(2)–S(1)	2.233 (12)	S(1)···S(2)	3.947 (15)	S(1)···S(4)	3.610 (12)
Fe(1)–S(6)	2.180 (10)	Fe(2)–S(3)	2.213 (10)	S(2)···S(3)	3.898 (13)	S(3)···S(4)	3.602 (12)
Fe(3)–S(3)	2.177 (10)	Fe(4)–S(5)	2.203 (10)	S(2)···S(5)	3.951 (13)	S(4)···S(5)	3.608 (12)
Fe(3)–S(5)	2.195 (10)	Fe(4)–S(6)	2.218 (10)	S(2)···S(6)	3.931 (13)	S(4)···S(6)	3.600 (12)
mean	2.187	mean	2.217	mean	3.932	mean	3.605
Fe(6)–S(1)	2.281 (11)	Fe(2)–S(2)	2.154 (11)	S(1)···S(3)	3.527 (14)	S(1)···S(6)	4.096 (13)
Fe(6)–S(3)	2.255 (11)	Fe(4)–S(2)	2.182 (10)	S(5)···S(6)	3.490 (13)	S(3)···S(5)	4.080 (13)
Fe(5)–S(5)	2.261 (11)	mean	2.168	mean	3.508	mean	4.088
Fe(5)–S(6)	2.241 (11)						
mean	2.260						
S(2)–Fe(2)–S(1)	128.2 (4)	S(4)–Fe(1)–S(1)	109.8 (4)	P(2)–Fe(2)–S(2)	89.8 (4)	P(1)–Fe(1)–S(4)	100.0 (4)
S(2)–Fe(2)–S(3)	126.4 (5)	S(4)–Fe(1)–S(6)	110.0 (4)	P(4)–Fe(4)–S(2)	90.8 (4)	P(3)–Fe(3)–S(4)	98.4 (4)
S(2)–Fe(4)–S(6)	126.6 (5)	S(4)–Fe(3)–S(3)	110.6 (4)	mean	90.3	mean	99.2
S(2)–Fe(4)–S(5)	128.6 (4)	S(4)–Fe(3)–S(5)	110.2 (4)	P(1)–Fe(1)–S(1)	92.1 (4)	Cl(1)–Fe(5)–S(5)	116.7 (5)
mean	127.5	mean	110.2	P(1)–Fe(1)–S(6)	91.2 (4)	Cl(1)–Fe(5)–S(6)	115.7 (5)
S(4)–Fe(5)–S(5)	103.6 (4)	S(1)–Fe(1)–S(6)	138.7 (4)	P(2)–Fe(2)–S(1)	92.1 (4)	Cl(2)–Fe(6)–S(1)	118.0 (5)
S(4)–Fe(5)–S(6)	103.9 (4)	S(3)–Fe(3)–S(5)	137.9 (4)	P(2)–Fe(2)–S(3)	94.4 (4)	Cl(2)–Fe(6)–S(3)	115.0 (4)
S(4)–Fe(6)–S(1)	102.6 (4)	mean	138.3	P(3)–Fe(3)–S(3)	92.3 (4)	Cl(1)–Fe(5)–S(4)	113.5 (4)
S(4)–Fe(6)–S(3)	103.1 (4)			P(3)–Fe(3)–S(5)	91.7 (4)	Cl(2)–Fe(6)–S(4)	114.1 (4)
mean	103.3			P(4)–Fe(4)–S(5)	92.7 (4)	mean	115.5
S(1)–Fe(2)–S(3)	105.0 (4)			P(4)–Fe(4)–S(6)	94.1 (4)		
S(5)–Fe(4)–S(6)	104.3 (4)			mean	92.6		
S(5)–Fe(5)–S(6)	101.7 (4)						
S(1)–Fe(6)–S(3)	102.1 (4)						
mean	103.3						

$[\text{Fe}_4\text{S}_4\text{Br}_4]^{2-}$, and 3 (with $[\text{Fe}_6\text{S}_6\text{Br}_6]^{3-}$) afforded $\text{Fe}_6\text{S}_6(\text{PET}_3)_4\text{Br}_2$, which is prepared in better yields (57%, 65%) in the last two reactions. Reactions analogous to (1) and (2) gave $\text{Fe}_6\text{S}_6(\text{PET}_3)_4\text{Cl}_2$, provided in much higher yield (84%) by the core expansion reaction (2). These compounds have very distinctive ^1H NMR spectra (Figure 1) in which the methyl and methylene protons of the phosphine ligands experience upfield (positive) isotropic shifts induced by the $S = 1$ ground states of the clusters.⁴³ The methylene shifts are clearly very sensitive to the nature of the core chalcogenide and the halide. Also prepared by similar means were $\text{Fe}_6\text{S}_6(\text{PMe}_3)_4\text{Cl}_2$, $\text{Fe}_6\text{S}_6(\text{P-}n\text{-Bu}_3)_4\text{Cl}_2$, and $\text{Fe}_6\text{S}_6(\text{PET}_3)_4\text{I}_2$. Their NMR spectra conform to the pattern of Figure 1, showing that they have the same structure. The presence of two pairs of equivalent phosphines is consistent with one of two isomers based on the prismane core, the only known Fe_6S_6 core prior to the present work.⁴⁴ The structure of the representative complex $\text{Fe}_6\text{S}_6(\text{P-}n\text{-Bu}_3)_4\text{Cl}_2$ was determined by X-ray diffraction. Despite extensive attempts, we were unable to obtain diffraction-quality crystals of any other compound in the set.

Structure of $\text{Fe}_6\text{S}_6(\text{P-}n\text{-Bu}_3)_4\text{Cl}_2$. This compound crystallizes in tetragonal space group $I4_1$ with one molecule in the asymmetric unit. The n -butyl groups exhibit extensive thermal motion but are otherwise unexceptional and are not considered further. Two views of the $\text{Fe}_6\text{S}_6\text{P}_4\text{Cl}_2$ portion of the molecule are provided in Figure 3, and selected metric data are set out in Table V. Not included in this table is the large set of Fe–S–Fe angles,³³ all of which occur in the interval 71 – 76° , which is normal for Fe–S clusters.¹ The present cluster presents a stereochemistry unprecedented in transition-element chalcogenide chemistry and is the first example of an Fe–S cluster not constructed in its entirety

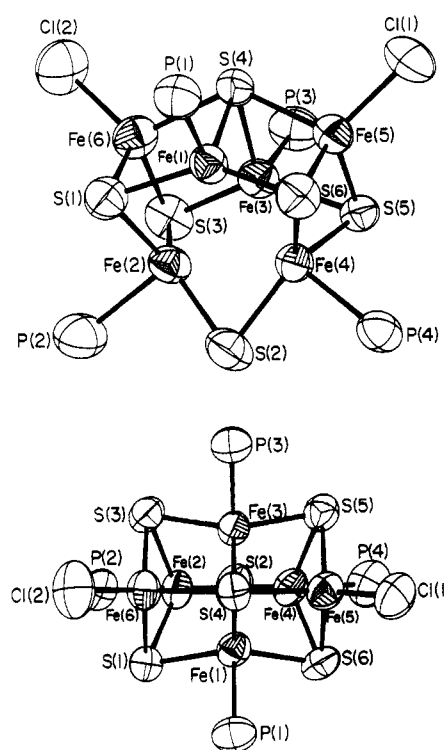


Figure 3. Structure of the $\text{Fe}_6\text{S}_6\text{P}_4\text{Cl}_2$ portion of $\text{Fe}_6\text{S}_6(\text{P-}n\text{-Bu}_3)_4\text{Cl}_2$, showing 50% probability ellipsoids and the atom-labeling scheme. The lower view is down the idealized C_2 axis, containing S(2,4).

(43) Snyder, B. S.; Reynolds, M. S.; Papaefthymiou, G. C.; Frankel, R. B.; Holm, R. H., results to be submitted for publication.

(44) Excluded from this statement is the core of $[\text{Fe}_6\text{S}_6(\text{CO})_{12}]^{2-}$, which represents a case in which the metal atoms do not form an "open" or closed polyhedron. The cluster is composed of two $[\text{Fe}_2\text{S}_2(\text{CO})_6]^{2-}$ ligands bound to a central $[\text{Fe}_2\text{S}_2]^{2+}$ core: Lilley, G. L.; Sinn, E.; Averill, B. A. *Inorg. Chem.* **1986**, *25*, 1073.

by the fusion of Fe_2S_2 rhombs. It and $[\text{Fe}_6\text{S}_9(\text{SR})_2]^{4-}$ are the only examples of Fe–S clusters that exhibit three bridging modalities, μ_2 -S, μ_3 -S, and μ_4 -S. Finally, it is the fourth entry into the family of 6-Fe(S) clusters and can be rationally added to a scheme of topological transformations that interrelate these clusters.

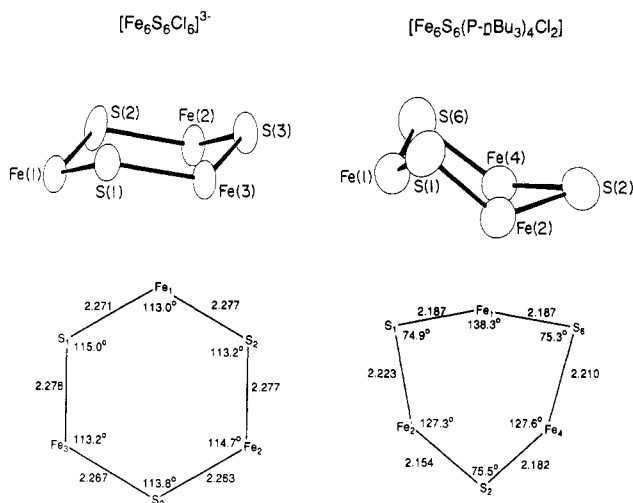


Figure 4. Comparison of the conformations and dimensions of the chairlike Fe_3S_3 rings in $[\text{Fe}_6\text{S}_6\text{Cl}_6]^{3-}$ (PPN⁺ salt) and $\text{Fe}_6\text{S}_6(\text{P-}n\text{-Bu}_3)_4\text{Cl}_2$.

The $[\text{Fe}_6(\mu_2\text{-S})(\mu_3\text{-S})_4(\mu_4\text{-S})]^{2+}$ core, which formally contains 4 Fe(II) + 2 Fe(III), is built by the fusion of six nonplanar Fe_2S_2 rhombs to form an open basket with the bridging group Fe(2)–($\mu_2\text{-S}(2)$)–Fe(4) as the handle with a bond angle of 75.5° . This results in the presence of two confacial Fe_3S_3 rings or “open faces”, each in a chairlike configuration. The conformation and dimensions of one of these rings are shown in Figure 4, where they are compared with those of the prismane $[\text{Fe}_6\text{S}_6\text{Cl}_6]^{3-}$. Any metal-binding propensity of the clusters $\text{Fe}_6\text{E}_6(\text{PR}_3)_4\text{X}_2$ would utilize one or both open faces. Such a process would be similar to the capping reactions of prismanes, thus far accomplished with $\text{Mo}(\text{CO})_3$ and $\text{W}(\text{CO})_3$ fragments.¹⁸ Comparison of open faces of the basket and prismane cores shows that the former have much larger internal angles at the Fe atoms and attendant relatively long S...S separations of 3.93–4.10 Å. In prismanes, these distances are 3.59–3.63 Å in a representative case. It appears that the basket core is less well configured to bind a capping metal with the usual M–S bond lengths and normal S–M–S and M–($\mu_4\text{-S}$)–Fe angles near 90 and 75° , respectively. Owing to the presence of open faces, $\text{Fe}_6\text{S}_6(\text{P-}n\text{-Bu}_3)_4\text{Cl}_2$ is a member of the group of clusters containing opened metal polyhedra.⁴⁵

The close approach of the basket core to C_{2v} symmetry, under which the C_2 axis is coincident with the S(2)–S(4), vector, results in considerable regularity in the structure. Thus, the mean plane Fe(2,4,5,6)S(2,4)P(2,4)Cl₂ contains the core atoms to within ± 0.048 Å and the terminal atoms to within ± 0.157 Å. The mean plane Fe(1,3)S(2,4)P(1,3) is perfect to within ± 0.045 Å. Under C_{2v} symmetry there are three inequivalent Fe sites, all of which are four-coordinate. The Fe(5,6) sites binding chloride are quite normal. They have trigonally distorted tetrahedral symmetry, and the Fe atoms are placed 0.98 Å above the S_3 planes. Mean values of the Fe–Cl distances and Cl–Fe–S angles, 2.193 Å and 115.5° , respectively, are close to those in $[\text{Fe}_4\text{S}_4\text{Cl}_4]^{2-}$ ⁴⁶ (2.211 (2) Å, 114.9°). On the basis of bond distances in the latter and in $[\text{FeCl}_4]^{-2-}$,¹ these sites appear to be more oxidized than those containing PET_3 . The Mössbauer spectrum rules out trapped oxidation states.⁴³

Both types of phosphine-bound Fe atoms reside in coordination units that are quite similar and have been previously observed only for the $\text{M}(\text{PR}_3)_3\text{S}_3$ sites in $\text{Fe}_7\text{S}_6(\text{PET}_3)_4\text{Cl}_3$ ²⁰ and $\text{Co}_7\text{S}_6(\text{PPh}_3)_5\text{Cl}_2$.^{19b} In terms of average dimensions, the Fe atoms are only 0.113 Å above the S_3 plane and have one or two markedly obtuse S–Fe–S angles of 127.5 and 138.3° . The other angles of this type are normal (103.3°). The angles P–Fe–S cover the range 89.9 – 100.0° . These sites have the gross shape of a trigonal pyramid but are so distorted that they closely approach only C_s

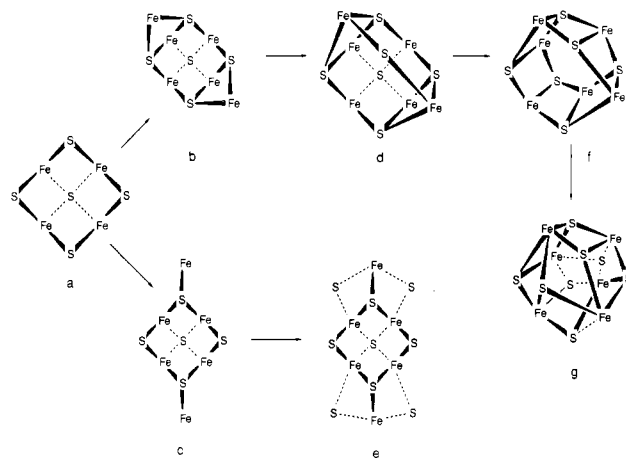


Figure 5. Scheme showing the formal buildup of 6-Fe cores from the fragment a by addition of Fe and S atoms. Cores d–g have been experimentally realized (see text).

symmetry with the mirror plane bisecting the unique S–Fe–S angle and containing the Fe–P bond. The mean Fe–P bond length of 2.309 Å is virtually indistinguishable from the corresponding distance in the Fe(III) cluster $[\text{Fe}_6\text{S}_6(\text{PET}_3)_6]^{2+}$ (2.293 Å) and in $\text{Fe}_7\text{S}_6(\text{PET}_3)_4\text{Cl}_3$ ²⁰ (2.289, 2.298 Å) and is about 0.07 Å shorter than that for $\text{Fe}(\text{PET}_3)_2\text{Br}_2$, where steric interactions probably influence metal–ligand bond lengths. Because of the differences in coordination environments and the lack of $\text{Fe}^{\text{II,III}}\text{-PR}_3$ bond lengths generally, the Fe–P separations are of no apparent value in inferring relative extents of oxidation in $\text{Fe}_6\text{S}_6(\text{P-}n\text{-Bu}_3)_4\text{Cl}_2$.

Within the core framework, Fe–S bond lengths are not exceptional. It need only be noted that bond lengths do not increase as the bridging multiplicity of a sulfur atom increases, a behavior found in $[\text{Fe}_6\text{S}_9(\text{SR})_2]^{4-}$ clusters.^{2–5} While the two distances Fe(2,4)–($\mu_2\text{-S}(2)$) are the shortest (mean 2.168 Å), Fe–($\mu_4\text{-S}$) distances essentially bracket those to $\mu_3\text{-S}$ atoms. Of more interest are the Fe–Fe distances, which overall tend to be shorter than in other mixed-valence Fe–S clusters. This does not apply to the longest such distance, Fe(1)–Fe(3) (2.835 (6) Å), which involves two atoms not in the same rhomb. The remaining 11 distances average to 2.672 (21) Å. We conclude that direct Fe–Fe bonding makes an important contribution to core stabilization and is partly responsible for the relatively small displacements of Fe atoms from their S_3 planes at phosphine binding sites. In contrast, Fe–Fe distances range from 2.746 (2) to 2.777 Å in $[\text{Fe}_4\text{S}_4\text{Cl}_4]^{2-}$,⁴⁶ 2.760 to 2.771 Å in $[\text{Fe}_6\text{S}_6\text{Cl}_6]^{3-}$,⁸ and 2.692 to 2.808 Å in $[\text{Fe}_6\text{S}_9(\text{SR})_2]^{4-}$.^{2–4} Another contributing factor to stability is the substitution pattern of terminal ligands. For $\text{Fe}_6\text{S}_6(\text{PR}_3)_4\text{X}_2$ there are six geometrical isomers (enantiomers excluded). In all but one of these, the phosphines are bound to Fe atoms in the *same* Fe_2S_2 rhomb. The structure unique in this sense is that observed here, and it is stabilized relative to the others by decreased ligand–ligand interactions assuming a roughly constant core structure.

Formal Buildup of Six-Iron Clusters. In the interest of providing a conceptual relationship amongst 6-Fe core structures by simple transformations, the scheme in Figure 5 is presented. When one starts with the central $\text{Fe}_4(\mu_4\text{-S})(\mu_2\text{-S})_4$ square fragment a of $[\text{Fe}_6\text{S}_9(\text{SR})_2]^{4-}$, addition of two Fe atoms can occur in only two chemically reasonable ways. In one mode, Fe atoms are added along opposite edges, converting all $\mu_2\text{-S}$ atoms to $\mu_3\text{-S}$ (b). In the other, Fe atoms are added to opposite $\mu_2\text{-S}$ atoms (c), leading to the disposition of Fe atoms observed in $[\text{Fe}_6\text{S}_9(\text{SR})_2]^{4-}$. Addition of one $\mu_2\text{-S}$ atom to fragment b generates the basket Fe_6S_6 core (d) of the present clusters, while incorporation of four such atoms into fragment c affords the Fe_6S_9 core (e). The topological conversion of basket Fe_6S_6 to prismane Fe_6S_6 (f) requires only two steps: cleavage of a single Fe–($\mu_4\text{-S}$) bond and bond formation between that Fe atom and $\mu_2\text{-S}$. Capping of the two open faces of the prismane with $\mu_3\text{-S}$ atoms completes formation of the $\text{Fe}_6(\mu_3\text{-S})_8$ core (g). Because the prismane core in principle or

(45) Albers, M. O.; Robinson, D. J.; Coville, N. J. *Coord. Chem. Rev.* **1986**, *69*, 127.

(46) Bobrik, M. A.; Hodgson, K. O.; Holm, R. H. *Inorg. Chem.* **1977**, *16*, 1851.

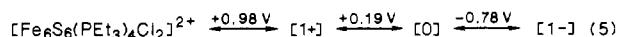
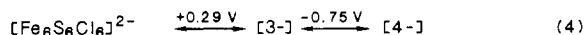
Table VI. Electrochemical Properties of Fe₆S₆ Clusters

cluster ^a	<i>v</i> , mV/s	oxidn			redn		
		<i>E</i> _{1/2} , V	Δ <i>E</i> _p , mV	<i>i</i> _{pa} / <i>i</i> _{pc}	<i>E</i> _{1/2} , V	Δ <i>E</i> _p , mV	<i>i</i> _{pc} / <i>i</i> _{pa}
Fe ₆ S ₆ (PEt ₃) ₄ Cl ₂	50	+0.18	85	1.0	-0.78	85	0.98
	200	+0.19 ^b	130	1.0	-0.78	115	0.98
Fe ₆ Se ₆ (PEt ₃) ₄ Cl ₂	50	+0.16	90	0.97			
	200	+0.16	125	0.97			
[Fe ₆ S ₆ Cl ₆] ³⁻	50	+0.28	100	1.0	-0.76 ^c		
	200	+0.29 ^d	140	1.0	-0.75 ^d	145	0.71

^a For the Cp₂Fe⁺⁰ couple under these conditions, *E*_{1/2} = +0.46 V and Δ*E*_p = 75 mV (50 mV/s), 100 mV (200 mV/s). ^b Additional oxidation at +0.98 V (series 5). ^c Irreversible. ^d The values +0.24 V (2-/3-) and -0.70 V (3-/4-) were reported with use of a Pt working electrode and 0.1 M (*n*-Bu₄N)ClO₄ supporting electrolyte; Δ*E*_p = 116 and 139 mV, respectively.^{8b}

in actuality¹⁸ can also be capped by metal atoms, successive capping of fragment *f* leads to the Fe₇S₆ and Fe₈S₆ cores as realized in Fe₇S₆(PEt₃)₄Cl₃²⁰ and [Fe₈S₆I₆]³⁻,¹³ respectively. This topological relationship between the three cores has been pointed out by us earlier.²⁰

Core Structure and Oxidation Level. The conversion d → f in Figure 5 emphasizes that the two cores, while isostoechiometric, are topologically inequivalent. They are also not isoelectronic in structurally determined cases but occur in compounds that are members of the electron-transfer series 4^{8b,10} and 5, illustrated



with chloride clusters. Clusters with isoelectronic cores are aligned vertically; half-wave potentials vs SCE measured by cyclic voltammetry at 200 mV/s in dichloromethane are indicated. Electrochemical data are summarized in Table VI.

Fe₆S₆(PEt₃)₄Cl₂ exhibits a chemically reversible (*i*_{pa}/*i*_{pc} ≈ 1) reduction at -0.78 V (140 mV) and oxidation at +0.19 V (130 mV). The indicated peak separations are much larger than the value Δ*E*_p = 59 mV for an electrochemically strictly reversible process, but in our experience they are not unusual for chemically reversible electron transfer in dichloromethane. Similar values are encountered for the oxidation and reduction of prismane clusters.^{8b} Note that Δ*E*_p = 140 mV for the couple [Fe₆S₆Cl₆]²⁻,³⁻ and that the prismane structure has been proven for [Fe₆S₆Cl₆]²⁻,⁹ as well as for [Fe₆S₆I₆]²⁻,¹¹ On this basis, it is unlikely that the rather large peak separations are associated with a chemical change. The peak current ratio for the couple [Fe₆S₆Cl₆]³⁻,⁴⁻ indicates some decomposition or alteration of the reduced cluster, but we did not detect any additional redox processes indicative of a new cluster species. A second oxidation of Fe₆S₆(PEt₃)₄Cl₂, at +0.98 V, is also chemically reversible.

Coulometric oxidation of the neutral cluster in series 5 is well-behaved, with *n* = 1.0, and affords a monocationic cluster isoelectronic with the 3- prismane. We have not yet established whether [Fe₆S₆(PEt₃)₄Cl₂]⁺ is sufficiently stable for isolation, in order to determine directly by X-ray methods if its core and the isoelectronic core in, e.g., [Fe₆S₆Cl₆]³⁻ have the same or different structure(s). The coulometric oxidation was performed over a 30-min period in a 2.5 mM solution in dichloromethane with a Pt-gauze electrode. Immediate examination of the oxidized solution revealed no processes other than those in series 5. Consequently, we regard it as improbable that [Fe₆S₆(PEt₃)₄Cl₂]⁺ has isomerized to a prismane core, at least over this time period. Attempts to crystallize this cluster are in progress.

Core Conversion and Related Reactions. As noted at the outset, Fe₇S₆(PEt₃)₄Cl₃²⁰ in solution spontaneously converts to a new paramagnetic cluster, whose identity was unknown at the time of the initial observation. We have established here by ¹H NMR that this cluster is in fact Fe₆S₆(PEt₃)₄Cl₂, formed in 95% yield after 22 h in a chloroform solution initially 5.6 mM in the original cluster. This process is reaction 6 in the scheme set out in Figure 6. In the reactions 2, 3, 6-8, and 12, discovered in this work, stoichiometric reactions cannot be provided owing to the formation of black insoluble byproducts, usually in rather small amounts, in each of these reactions. The term "core conversion" used in

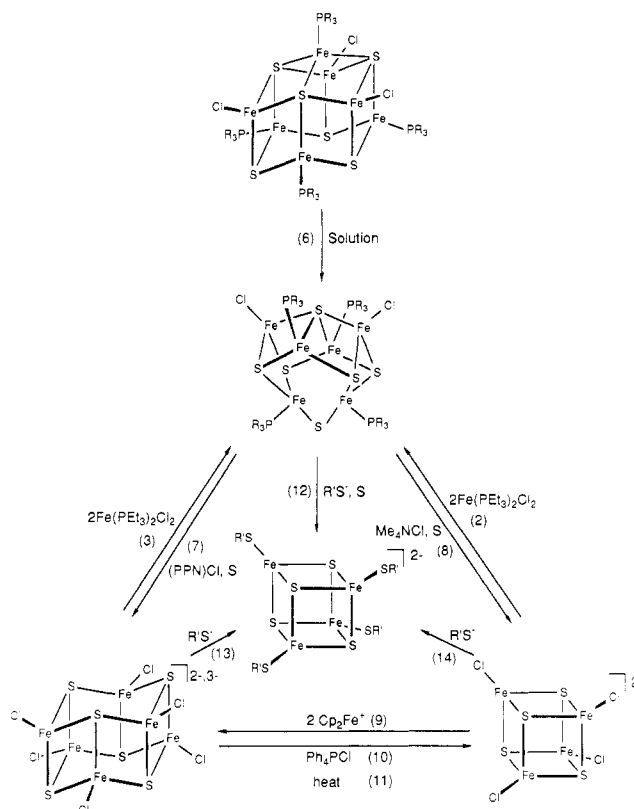


Figure 6. Schematic depiction of core conversion and related reactions of Fe₄S₄, Fe₆S₆, and Fe₇S₆ clusters (R = Et, R' = *p*-tol). Reactions 9⁹ and 10, 11, and 13⁸ have been established by other investigators.

this and earlier reports is intended to convey an overall increase or decrease in core nuclearity without implication of pathway. The reaction summaries below describe effective changes.

Core expansion reaction 2 involves the addition of two Fe(II) atoms to, and partial ligand substitution of, [Fe₄S₄Cl₄]²⁻ to yield Fe₆S₆(PEt₃)₄Cl₂. Reaction 3 is one of core isomerization induced by one-electron reduction and partial ligand substitution of the initial prismane cluster. The only previous Fe₄S₄ ↔ Fe₆S₆ conversions are reaction 9,⁹ the oxidative formation of a prismane cluster from a cubane (3[Fe₄S₄Cl₄]²⁻ - 2e⁻ → 2[Fe₆S₆Cl₆]²⁻), and the nonredox reverse reactions 10 and 11^{8b} induced by heat and chloride ion, respectively.

We have conducted reactions whose intent was to remove phosphine ligands, thereby changing the stereochemistry at those Fe sites to more nearly tetrahedral and causing the open faces to assume a configuration more conducive to binding. In reactions carried out in acetone with a 2.5:1 mole ratio of sulfur to phosphine and an equimolar ratio of chloride to phosphine, we find that phosphine is readily removed from Fe as Et₃PS but that the core is not stable. In reaction 7 three products were detected: [Fe₄S₄Cl₄]²⁻ (30%, in reaction mixture filtrate), [Fe₆S₆Cl₆]³⁻,⁸ (49%), and [Fe₂S₂]²⁻,²⁹ (6%). Yields of the last two clusters refer to isolated PPN⁺ salts. We did not consider the spectroscopic or electrochemical properties of the second product decisive for

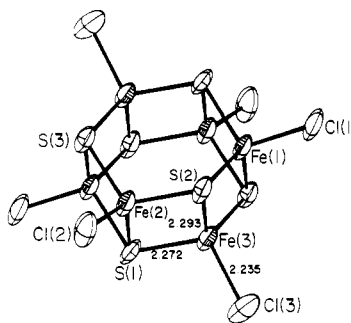


Figure 7. Structure of $[\text{Fe}_6\text{S}_6\text{Cl}_6]^{3-}$ as its PPN^+ salt, showing 50% probability ellipsoids, the atom-labeling scheme, and selected mean bond distances (Å).

identification and characterized the compound as $(\text{PPN})_3[\text{Fe}_6\text{S}_6\text{Cl}_6]$ by X-ray crystallography. The structure of the anion, which has imposed centrosymmetry and takes the form of a slightly distorted hexagonal prism, is shown in Figure 7. Metric data³³ are in reasonable conformance with corresponding dimensions found in the Et_4N^+ salt;^{8b} mean Fe-Fe and Fe-S distances are 2.791 and 2.279 Å, respectively. In a parallel experiment, reaction 8 afforded a 46% yield of $[\text{Fe}_4\text{S}_4\text{Cl}_4]^{2-}$ as its Me_4N^+ salt, thus confirming its formation in a reaction system containing sulfur and chloride. In reactions 7 and 8 cations were chosen to trap clusters as sparingly soluble salts in acetone. In each reaction, complete or nearly complete removal of phosphine from the starting cluster as Et_3PS was demonstrated by ^{31}P NMR. Of the iron content of the initial cluster in reaction 7, 85% is accounted for in identified products; at least part of the remainder occurs in an insoluble black material not further examined.

In a final experiment, reaction 12 (Figure 6), $\text{Fe}_6\text{S}_6(\text{PET}_3)_4\text{Cl}_2$ in acetonitrile was reacted with 6 equiv each of sulfur and *p*-toluenethiolate in order to learn if a cluster with only thiolate terminal ligands could be prepared. Instead, $(\text{Me}_4\text{N})_2[\text{Fe}_4\text{S}_4(\text{S}$

p-tol)₄] was isolated in small yield (17%). The outcome of this reaction is somewhat similar to that of reaction 13, wherein the initially formed prismane thiolate cluster $[\text{Fe}_6\text{S}_6(\text{SR})_6]^{3-}$ rapidly transforms in a nonredox process to $[\text{Fe}_4\text{S}_4(\text{SR})_4]^{2-}$,^{8b,10} which is also accessible in high yield by the oft-utilized ligand substitution reaction 14.²³ In the present reaction, sulfur presumably acts as an oxidant, leading to formation of the stable cubane cluster. Reaction of $\text{Fe}_6\text{S}_6(\text{PET}_3)_4\text{Cl}_2$ and thiolate affords the new clusters $\text{Fe}_6\text{S}_6(\text{PET}_3)_4(\text{SR})_2$,²¹ which will be reported subsequently.

Summary. This research has resulted in the synthesis of a new group of iron-sulfur clusters of general formulation $\text{Fe}_6\text{S}_6(\text{PR}_3)_4\text{X}_2$ (X = halide), which contain the previously unknown basketlike core $[\text{Fe}_6\text{S}_6]^{2+}$. Full structural details of a representative cluster are provided. Current evidence suggests that, at least over short times, isoelectronic prismane and basket cores are stable and do not interconvert spontaneously. Triethylphosphine may be efficiently removed from the clusters with sulfur. Reaction products have either the prismane or cubane structures. This observation suggests that the basket configuration may be dependent on the presence of phosphine ligands and, therewith, distorted-trigonal-pyramidal coordination units and relatively short Fe-Fe separations. These clusters feature open core faces in the form of chairlike Fe_3S_3 rings, which may not be configured ideally for capping by metals. The metal-binding propensities of $\text{Fe}_6\text{S}_6(\text{PR}_3)_4\text{X}_2$ clusters in the presence and absence of sulfur or other reagents introduced to remove phosphine ligands are under examination.

Acknowledgment. This research was supported by NIH Grant GM 28856. X-ray diffraction equipment was obtained by NIH Grant 1 S10 RR02247.

Supplementary Material Available: Tables of atom positional and thermal parameters, bond distances and angles, and calculated hydrogen atom positions for $\text{Fe}(\text{PET}_3)_2\text{Br}_2$, $\text{Fe}_6\text{S}_6(\text{PET}_3)_4\text{Cl}_2$, and $(\text{PPN})_3[\text{Fe}_6\text{S}_6\text{Cl}_6]$ and a stereoview of $\text{Fe}_6\text{S}_6(\text{P}-n\text{-Bu}_3)_4\text{Cl}_2$ (24 pages); tables of calculated and observed structure factors (74 pages). Ordering information is given on any current masthead page.

Contribution from Department of Chemistry and Laboratory for Molecular Structure and Bonding, Texas A&M University, College Station, Texas 77843

Further Studies of Bi-Oxo-Capped Triniobium Cluster Complexes

F. Albert Cotton,* Michael P. Diebold, and Wieslaw J. Roth

Received December 14, 1987

Synthetic and structural studies that substantially extend our knowledge of $\text{Nb}_3(\mu_3\text{-O})_2$ complexes are reported. Treatment of $\text{Nb}_2\text{Cl}_6(\text{THT})_3$ (THT = tetrahydrothiophene) with oxygen-free H_2SO_4 in $\text{H}_2\text{O}/\text{THF}$ or an acetic acid/acetic anhydride mixture, followed by suitable workup procedures, allows the isolation of compounds containing the $[\text{Nb}_3(\mu_3\text{-O})_2(\text{SO}_4)_6(\text{H}_2\text{O})_3]^{3-}$ and $[\text{Nb}_3(\mu_3\text{-O})_2(\text{O}_2\text{CCH}_3)_6(\text{THF})_3]^+$ ions. The former was obtained as the compound $(\text{NH}_4)_3(\text{H}_3\text{O})_2[\text{Nb}_3\text{O}_2(\text{SO}_4)_6(\text{H}_2\text{O})_3]\cdot n\text{H}_2\text{O}$ (1), which forms blocky monoclinic crystals, and as a related compound of uncertain cation content, which forms acicular hexagonal crystals. The structure of the latter was solved and refined (space group $P6_3/m$) to the point of showing clearly the complex trinuclear anion but with an intractably disordered array of cations. The monoclinic form was fully characterized by X-ray crystallography: $P2_1/m$ with $a = 9.651$ (3) Å, $b = 9.866$ (3) Å, $c = 16.141$ (5) Å, $\beta = 94.07$ (3)°, $V = 1533$ (2) Å³, and $Z = 2$. The mean Nb-Nb distance is 2.870 [6] Å, and the mean Nb-($\mu_3\text{-O}$) distance is 2.030 [2] Å. The acetate was isolated as orthorhombic crystals ($Pnma$) of $[\text{Nb}_3\text{O}_2(\text{O}_2\text{CCH}_3)_6(\text{C}_4\text{H}_8\text{O})_3][\text{NbOCl}_4(\text{C}_4\text{H}_8\text{O})]$ (2), with unit cell dimensions $a = 14.425$ (5) Å, $b = 16.662$ (4) Å, $c = 19.423$ (8) Å, $V = 4668$ (5) Å³, and $Z = 4$. The mean Nb-Nb and Nb-($\mu_3\text{-O}$) distances are 2.831 [3] and 2.019 [3] Å, respectively. The $[\text{NbOCl}_4(\text{C}_4\text{H}_8\text{O})]^-$ ion has Nb=O = 1.682 (9) Å, Nb-O_{THF} = 2.384 (11) Å, and a mean Nb-Cl distance of 2.385 [2] Å. A byproduct in the preparation of 2 is $\text{Nb}_2\text{Cl}_2(\text{OEt})(\text{O}_2\text{CMe})_5$ (3), which has a novel structure in which two $(\eta^2\text{-CH}_3\text{CO}_2)_2\text{Nb}$ groups are joined by $\mu\text{-OC}_2\text{H}_5$, two $\mu\text{-Cl}$ atoms, and $\mu_2\text{-}\eta^2\text{-CH}_3\text{CO}_2$. The Nb-Nb distance, 2.789 (1) Å, is consistent with the presence of a single bond. Crystal data for 3: space group $P2_1/n$, $a = 10.057$ (1) Å, $b = 14.912$ (3) Å, $c = 13.880$ (2) Å, $\beta = 103.67$ (1)°, $V = 2022$ (1) Å³, $Z = 4$.

Introduction

Since the discovery¹ and the subsequent elucidation and development of the chemistry² of the trimeric bicapped M_3X_{17} clusters of molybdenum and tungsten, of the formula $[\text{M}_3\text{X}_2(\text{O}_2\text{CR})_6\text{L}_3]^{n+}$, the existence of such clusters appeared to be limited

to these group 6 metals. While trinuclear hexacarboxylates of many other transition elements are known, they are oxo centered with a planar M_3O group³ and have no M-M bonding. It was discovered⁴ in 1980 that a novel niobium sulfate compound, first

(1) Bino, A.; Cotton, F. A.; Dori, Z.; Koch, S.; Küppers, H.; Millar, M.; Sekutowski, J. C. *Inorg. Chem.* 1978, 17, 3245.
(2) Cotton, F. A. *Polyhedron* 1986, 5, 3.

(3) (a) Mehrotra, R. C.; Bohra, R. *Metal Carboxylates*; Academic: New York, 1983. (b) Yuansheng, Jiang; Aoaing, Tang; Hoffman, R.; Jinling, Huang; Jiayi, Lu. *Organometallics* 1985, 4, 27.
(4) Bino, A. *J. Am. Chem. Soc.* 1980, 102, 7990.